Soft Matter

Cite this: *Soft Matter*, 2012, **8**, 9436

www.rsc.org/softmatter

PAPER

Smart hydrogels based on responsive star-block copolymers†

Alexander Schmalz, Holger Schmalz* and Axel H. E. Müller*

Received 25th March 2012, Accepted 3rd May 2012
DOI: 10.1039/c2sm25686j

A series of smart hydrogels based on dual stimuli responsive star-block copolymers responding to pH and temperature were prepared *via* atom transfer radical polymerization (ATRP) employing the core-first method. They consist of poly(2-(dimethylamino)ethyl methacrylate) (PDMA) inner blocks and outer blocks comprised of poly(di(ethylene glycol) methyl ether methacrylate) (PDEGMA). The aggregation behavior of these block copolymer stars is analyzed by dependence on block length and arm number. The dual stimuli responsiveness of the stars is demonstrated by turbidity as well as dynamic light scattering on dilute aqueous solution, and the gelation behavior of concentrated aqueous solutions is studied by rheology. Above the transition temperature of the PDEGMA outer blocks the stars form flower-like aggregates in dilute solution or free-standing gels at higher concentrations. When the temperature is increased further above the transition temperature of the PDMA inner block, the aggregates start to contract and a weakening was observed for soft gels, whereas for strong gels no influence on the moduli was detected. The behavior is controlled by both concentration and pH value. In addition, we show that the minimum polymer concentration for gel formation can be lowered by quaternizing the inner block of the stars, but a second response to stimuli is lost during the procedure.

Introduction

Hydrogels are three-dimensional hydrophilic networks that can bind a large amount of water or biological fluid.[1,2] Stimuli responsive hydrogels, *i.e.*, hydrogels responding with a large property change on small variations in their physical and/or chemical environment, have gathered much interest for their use as biomaterials, with applications such as controlled drug release, cell carriers and tissue engineering.[1–5] In general, hydrogels can be classified into two categories depending on their cross-linking method: chemical or physical. The network is usually built of water-soluble macromolecular chains connected either through permanent covalent bonds (chemical cross-linking) or through temporary junction points (physical cross-linking). Chemically crosslinked gels can consist of water-soluble polymers or of polymers that respond to external stimuli such as temperature or pH. Hydrogels based on cross-linked poly(*N*-isopropylacrylamide) (PNIPAAm) have been studied extensively because its lower critical solution temperature (LCST) is around 32 °C in water, making it a promising candidate for biomedical applications.[6–10] A physical gel typically consists of block copolymers where the stimuli responsive blocks are used to form the temporary crosslinking points, *i.e.*, the responsive block is switched insoluble by increasing its hydrophobic interactions. This can be based on a variety of triggers, such as temperature, pH, light, redox reactions or host–guest interactions.[11,12] It is noted that physical gels can be formed by low molecular weight gelators, too; however these systems are not within the scope of this contribution. One reason that much attention is being paid to physical hydrogels is because of their potential for biomedical applications, *e.g.* injectable hydrogels for drug delivery or tissue engineering.[13] However, in most physical hydrogels the "smart" component is only responsible for the formation/disintegration of the gel, most commonly seen in the form of ABA triblock copolymers where the B block merely provides solubility.[14,15] The easiest way to introduce dual stimuli responsiveness is to copolymerize thermo-sensitive monomers with monomers that are also sensitive to other triggers. This can be achieved by random copolymerization with a pH-responsive monomer like acrylic acid,[16,17] but advances in synthetic protocols have led to more efforts into block-type structures. Until now only a limited number of double temperature-sensitive ABC triblock terpolymers have been synthesized,[18,19] as well as dual temperature- and pH-sensitive ABA triblock copolymers[20–22] and ABC triblock terpolymers.[23] The same advances in synthesis have also opened the way to a more complete control over the polymer architecture, leading to increased interest in *e.g.* star-shaped polymers. Recent publications indicate that a star-shaped gelator is superior to its linear triblock counterpart, *i.e.*, they have a lower critical gelation concentration (cgc).[24,25]

Makromolekulare Chemie II, Universität Bayreuth, D-95440 Bayreuth, Germany. E-mail: holger.schmalz@uni-bayreuth.de; axel.mueller@uni-bayreuth.de

† Electronic supplementary information (ESI) available: ^{1}H-NMR spectra of $(DMA_{150}DEGMA_{100})_4$ and quaternized $(qDMA_{150}DEGMA_{100})_4$; μDSC traces for $(DMA_{130}DEGMA_{140})_6$ and $(DMA_{130}DEGMA_{60})_6$; additional DLS measurements and rheology data for $(DMA_nDEGMA_m)_x$ and $(qDMA_nDEGMA_m)_x$. See DOI: 10.1039/c2sm25686j

Our group has shown that linear and star-shaped poly-(2-(dimethylamino)ethyl methacrylate) (PDMA) as well as poly(2-(diethylamino)ethyl methacrylate) (PDEA) homopolymers are responsive to both pH and temperature.[27–29] We have recently made a first attempt to create double stimuli responsive hydrogels from star-shaped block copolymers $(A_nB_m)_x$, in which the A block is PDMA and the B block is comprised of PDEA.[26] However, the gelation behavior turned out to be very complex, due to the double responsive nature of both blocks. Thus, we decided to replace the outer block of the $(A_nB_m)_x$ star-block copolymers with a polymer that is responsive to temperature only.

Recently, more and more attention has been given to a new class of thermo-responsive polymers, the poly(oligo(ethylene glycol) methyl ether methacrylate)s (POEGMAs). By copolymerizing different OEGMAs, *i.e.*, methacrylates with different numbers of ethylene glycol units in the side chain, such as di(ethylene glycol) methyl ether methacrylate (DEGMA) and OEGMA with 8.5 ethylene glycol units, the cloud point of the copolymer can be tuned according to the molar ratio of the two monomers between 26 °C for pure PDEGMA and 90 °C for pure POEGMA.[30–32] These polymers have proven to be very versatile and have been applied in sensors,[33] polymer–protein conjugates,[34] photo-crosslinkable polymers[35] and the modification of natural polymers.[36] There have already been efforts to directly create chemically cross-linked gels from PDEGMA[37,38] as well as using PDEGMA and PDMA as stimuli responsive blocks in combination with other monomers. PDMA-*b*-PDEGMA-*b*-PDMA block copolymers[39] have been reported as well as double-responsive ABC triblock terpolymers where the C block was either P(DEGMA-*co*-OEGMA) or PDMA.[40] There has also been work published on star-shaped gelators with PDMA as the responsive outer block.[41]

In this paper we combine these approaches to create new hydrogels based on star-shaped block copolymers consisting of an outer block of thermo-responsive PDEGMA and an inner block of thermo- and pH-responsive PDMA. We propose that gel formation takes place according to an open association mechanism, with a sequential collapse of the blocks starting from the outside upon an increase in temperature. The collapse of the inner PDMA block is controlled by the pH value of the solution, *i.e.*, the gel can change its mechanical properties depending on the pH. This mechanism is illustrated in Scheme 1. Another possibility to utilize the PDMA block is quaternization to turn the inner block into a permanent cationic polyelectrolyte. This should lead to an increase in hydrophilicity along with a stretching of the inner block, *i.e.*, an increased volume fraction of the stars in solution, and eliminate the pH-responsiveness.

Experimental

Materials

Ethyl 2-bromoisobutyrate, *N*,*N*,*N*′,*N*″,*N*‴,*N*‴-hexamethyltriethylenetetramine (HMTETA), copper(I) chloride, 1,3,5-trioxane, iodomethane, and trimethylsilyldiazomethane were purchased from Aldrich and used without further purification. The solvents used were of p.a. quality. The monomers 2-(dimethylamino)ethyl methacrylate (98%, Aldrich) and di(ethylene glycol) methyl ether methacrylate (95%, Aldrich) were destabilized before use by passing through a basic alumina column. The synthesis of the sugar-based initiators with 5 and 8 2-bromoisobutyryl initiation sites, based on glucose and saccharose, respectively, is described in a previous publication.[42] For dialysis, regenerated cellulose membranes (ZelluTrans with MWCO 4000–6000) were used.

Synthesis of star shaped block copolymers

The identical PDMA precursor stars were used as in our previous work, which were synthesized by ATRP with sugar-based initiators.[26]

For the second block the same procedure was applied, except that acetonitrile was used as the solvent instead of anisole. The change of the solvent was necessary to achieve a high blocking efficiency. In a typical reaction 2 g of the 4-arm star PDMA macroinitiator (~0.084 mmol initiation sites), 4.7 g of the monomer di(ethylene glycol) methyl ether methacrylate (0.025 mol), 16.6 mg Cu(I)Cl (0.168 mmol), 38.7 mg HMTETA (0.168 mmol) and acetonitrile (31.2 g) as solvent were used. The catalyst complex solution was pumped into the reaction vessel, a screw cap vial equipped with a rubber septum, using a double-tipped metal needle with about 0.5 bar of nitrogen pressure to avoid contact with air. The polymerizations were carried out at 50 °C. All reactions for the second block were performed using a fixed ratio between monomer, initiation sites, catalyst and ligand of $[M]_0 : [I]_0 : [Cat] : [L] = 100 : 1 : 2 : 2$ at $[M]_0 \approx 0.063$ mol L^{-1}.

The arms of the resulting PDMA-*b*-PDEGMA star-block copolymers were cleaved off by an alkaline ester hydrolysis at elevated temperatures, using a procedure adapted from Plamper *et al.*[27] To circumvent the pH independent LCST of the PDEGMA block in water, a method in a non-aqueous solvent was chosen. The cleaving reaction was carried out in 1 M potassium hydroxide solution in methanol (1 M KOH in MeOH) at 70 °C. The product of this reaction for both the PDMA and PDEGMA blocks is poly(methacrylic acid) (PMAA), as the pendant side groups get hydrolyzed under the applied conditions. The obtained PMAA was transformed to poly(methyl methacrylate) (PMMA)

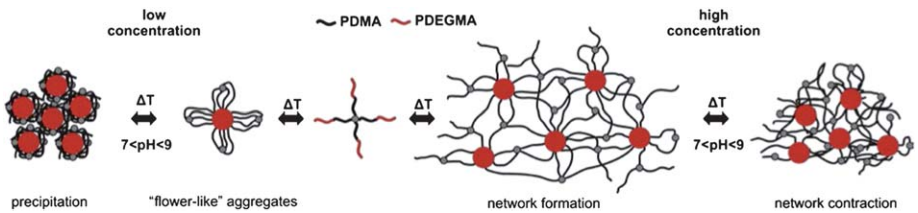

Scheme 1 Aggregation and network formation of dual temperature and pH responsive star-block copolymers in dependence on concentration.

using trimethylsilyldiazomethane to facilitate molecular characterization. The actual arm number of the precursor PDMA stars was calculated by comparing the theoretical arm length, obtained from conversion, with the experimental M_n of the cleaved arms obtained from MALDI-ToF. The block length of the PDEGMA block was calculated from NMR measurements by comparing the signal of the methoxy group of DEGMA with the signal of the dimethylamino group of DMA. The cleaved-off arms of the block copolymer stars were used to confirm the blocking efficiency as being close to unity.

The quaternization of the PDMA block of the star-block copolymers was carried out in a 0.5% w/w solution in acetone. Iodomethane was used as the quaternization agent, in a 1.5 fold excess compared to amino groups. The reaction was stirred overnight at room temperature and the precipitated product was centrifuged off and washed three times with pure acetone.

^{1}H-NMR spectroscopy

All measurements were performed with a Bruker Avance 300 spectrometer using deuterated chloroform or deuterium oxide as solvent.

MALDI-ToF mass spectrometry

MALDI-ToF MS measurements were performed on a Bruker Daltonics Reflex III instrument equipped with an N_2 laser (λ_0 = 337 nm) and applying an acceleration voltage of 20 kV in positive mode. Sample preparation was done according to the "dried-droplet" method. In detail, matrix (*trans*-3-indoleacrylic acid, IAA, conc. 2 mg mL^{-1}) and analyte (conc. 10 mg mL^{-1}) were separately dissolved in THF, subsequently mixed in a ratio of 20 : 5 μL. 1.5 μL of the final mixture was applied to the target spot and left to dry under air.

Size exclusion chromatography (SEC)

The apparent molecular weight distributions of the star-shaped homo- and copolymers were determined by SEC using dimethylacetamide (DMAc) with 0.05% lithium bromide as eluent at a flow rate of 0.8 mL min^{-1}. The equipment consisted of one pre-column and two analytical columns (PSS GRAM, 10^2 and 10^3 Å pore size, 7 μm particle size) and an Agilent 1200 RI detector. The measurements were performed at 60 °C.

The PMMA samples obtained from the arm cleavage were analyzed using a THF-SEC with a flow rate of 1 mL min^{-1}. This setup was equipped with one pre-column, four analytical columns (PSS SDV, 10^2, 10^3, 10^4 and 10^5 Å pore size, 5 μm particle size) and a Shodex 101 RI detector. The measurements were performed at 40 °C. For data evaluation a calibration with linear PMMA standards was used in all cases.

Cloud point measurements

The temperature-dependent solution behavior was investigated using a titrator (Titrando 809, Metrohm) equipped with a turbidity probe (Spectrosense, Metrohm, λ_0 = 523 nm) and a temperature sensor (Pt1000, Metrohm). The cloud points (T_{cl}) were determined by dissolving 30 mg of polymer in 30 mL of buffer solutions ranging from pH 7 to pH 9 (NIST buffer, Titrinorm VWR). The solutions were degassed by applying vacuum (50–100 mbar) for 15 min at room temperature in order to minimize bubble formation during the experiments. The measurements were performed using a homemade thermostattable vessel and for the experiments a constant heating rate of 1 K min^{-1} was applied using a thermostat (Lauda Ecoline Star-edition RE 306, ±0.01 °C). The cloud points were determined from the intersection of the two tangents applied to the two linear regimes of the transmittance curve at the onset of turbidity.

Dynamic light scattering

DLS was performed on an ALV DLS/SLS-SP 5022F compact goniometer system with an ALV 5000/E cross-correlator and a HeNe laser (λ_0 = 632.8 nm). The solutions were prepared by dissolving 2 mg of polymer in 2 mL of buffer solution of either pH 7 or 8 (NIST buffer, Titrinorm, VWR) and filtered prior to the measurements with 0.45 μm syringe filters (cellulose acetate, Roth). For temperature-dependent measurements, the decaline bath of the instrument was thermostatted using a LAUDA Proline RP 845 thermostat. At each temperature the sample was equilibrated for 10 min prior to data acquisition, which was done five times for the duration of 60 s each. The autocorrelation functions were recorded individually and evaluated using 2nd order cumulant analysis.

Rheology

Rheology measurements were conducted using a Physica MCR 301 rheometer with a cone-and-plate shear cell geometry (D = 50 mm, cone angle = 1°). For the temperature-dependent measurements a frequency of 1 Hz, a heating rate of 0.5 K min^{-1} and a strain of 0.5%, which is inside the linear viscoelastic regime, were applied. The temperature was controlled by a Peltier element. For the isothermal frequency sweeps (10^{-2} to 10^2 Hz) the temperature was adjusted to the desired value by heating the sample at a rate of 0.5 K min^{-1}. The samples were prepared using a Ditabis Cooling-Thermomixer MKR13. The polymers were directly dissolved in water at different low pH values, *i.e.*, pH = 2 or 3, to produce solutions with final pH values of pH = 7 or 8, respectively. This procedure avoids additional pH adjustments after sample preparation, which would result in salt (NaCl) formation and consequently might influence the solution behavior of the polyelectrolyte blocks. The samples were shaken in the MKR13 at 10 °C for several hours up to several days until the polymer was completely dissolved and subsequently stored at 3 °C until use.

Micro-differential scanning calorimetry (μDSC)

The calorimetric measurements were performed with a Setaram μDSC III using closed "batch" cells at a scanning rate 0.5 K min^{-1}. Millipore water was used as the reference substance.

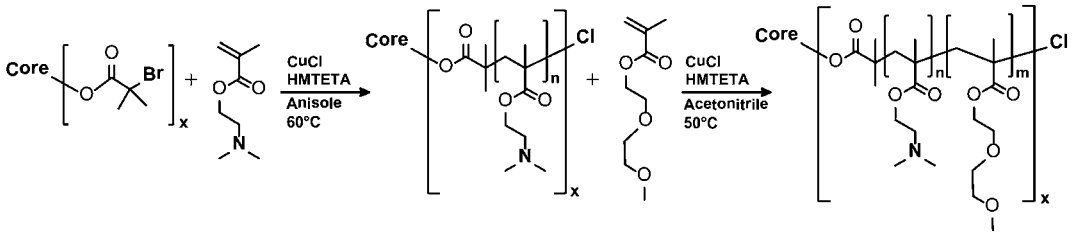

Scheme 2 Synthesis of $(DMA_nDEGMA_m)_x$ star-block copolymers.

Results and discussion

Synthesis and molecular characterization of star-block copolymers

We have synthesized star-shaped block copolymers consisting of a poly(2-(dimethylamino)ethyl methacrylate) (PDMA) inner block and a poly(di(ethylene glycol) methyl ether methacrylate) (PDEGMA) outer block. The synthesis was carried out with slight modifications according to a previously published protocol employing ATRP with halogen exchange and subsequent monomer addition. A grafting-from approach with functionalized sugar moieties was used.[26] This synthetic route is shown in Scheme 2. The synthetic protocol was tested using a monofunctional ATRP initiator, ethyl 2-bromoisobutyrate. Fig. 1 shows the SEC traces of the synthesized linear PDMA-*b*-PDEGMA block copolymer, $DMA_{75}DEGMA_{140}$, and the corresponding PDMA precursor. The trace of the precursor is monomodal with a narrow distribution (PDI = 1.13) while the block copolymer shows a small shoulder at higher elution volume but still has a reasonably narrow distribution (PDI = 1.32). This shoulder corresponds to a small amount of unreacted homopolymer but the peak of the block copolymer is completely shifted to a lower elution volume.

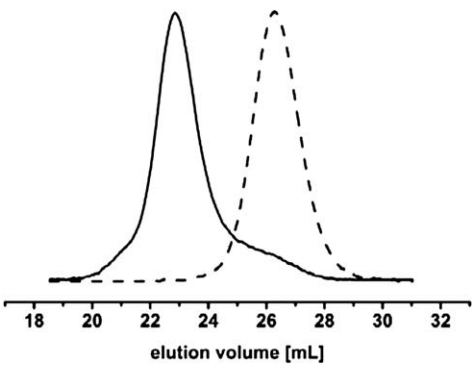

Fig. 1 SEC traces of the linear PDMA-*b*-PDEGMA block copolymer (solid line) and the corresponding PDMA precursor (dashed line).

We synthesized two homopolymer star precursors with different arm numbers but almost identical PDMA block lengths. The block lengths for the outer PDEGMA blocks were chosen to produce two different diblock copolymer stars from every precursor. This resulted in a total of 4 diblock copolymer stars with variations in arm number and the length of the outer block while keeping the length of the inner block almost constant.

All stars have narrow molecular weight distributions with PDIs ranging from 1.07 to 1.39 (Table 1). As an example, the SEC trace of the star $(DMA_{150}DEGMA_{100})_4$ is shown in Fig. 2a. The shoulder at low elution volume, *i.e.*, high molecular weight, indicates some star–star coupling. However, Fig. 2b shows a monomodal trace for the cleaved off arms of the star-block copolymer. This shows that the coupling process does not involve recombination of two chain-end radicals but rather the nucleophilic attack of an amino side group of the PDMA block on the chain end halogen. The pendant side groups of both blocks are cleaved off during the procedure and thus the chain coupling gets hydrolyzed, too, leading to the monomodal distribution.[26,43,44]

The molecular characterization of all star polymers is listed in Table 1. Later, the PDMA blocks of all stars were quaternized with iodomethane to yield a permanent strong polyelectrolyte block (PqDMA). The increased electrostatic repulsion and the osmotic pressure of the counterions inside the PqDMA block[45,46] should lead to a stretching of the arms. Consequently, the volume of the individual stars increases and causes the overall volume fraction of the stars in the solution to rise, which is supposed to result in a decrease of the critical gelation concentration. ^{1}H-NMR measurements were utilized to confirm the structure of the quaternized and nonquaternized block

Table 1 Molecular characteristics of the star-shaped $(DMA_nDEGMA_m)_x$ diblock copolymers and their gelation behavior

Polymer[a]	M_n[b] [10^3 g mol^{-1}]	PDI[c]	f_{DEGMA}[d]	Gelation behavior
$(DMA_{150}DEGMA_{40})_4$	125	1.39	0.21	No gelation
$(DMA_{130}DEGMA_{60})_6$	192	1.09	0.32	Free-standing gels
$(DMA_{150}DEGMA_{100})_4$	170	1.28	0.40	Free-standing gels
$(DMA_{130}DEGMA_{140})_6$	282	1.07	0.52	Free-standing gels

[a] $(DMA_nDEGMA_m)_x$: n and m are the number average degrees of polymerization of the respective blocks and x denotes the number average arm number as determined by a combination of MALDI-ToF MS and NMR. [b] Number average molecular weight of the stars as determined by a combination of MALDI-ToF MS and NMR. [c] Apparent polydispersity index as determined by SEC of the star polymers in DMAc. [d] Molar fraction of DEGMA units.

copolymer stars (see ESI, Fig. S1†). The NMR results were also used to calculate the block length of the outer PDEGMA block. The signals at 2.2 and 3.3 ppm, corresponding to the $-N(CH_3)_2$ and $-OCH_3$ groups, respectively, were compared to determine the PDEGMA block length, using the known block length of the inner PDMA block for signal calibration (see Experimental section). In the case of the quaternized stars, the signals from the peaks at 3.35 ppm and 3.2 ppm, corresponding to the $-O-CH_3$ and the $-N(CH_3)_2$ plus the $-N^+(CH_3)_3$ groups, respectively, were compared to determine the degree of quaternization of the PDMA blocks (~85%). The expected ratio for complete quaternization can be estimated from the ratio of block length determined from the spectrum of the nonquaternized stars. The difference between the expected ratio and the experimental ratio is the quaternization efficiency.

Aggregation of $(DMA_nDEGMA_m)_x$ diblock copolymer stars in dilute solution

The temperature and pH responsive nature of the star-block copolymers was investigated by turbidity measurements first. Fig. 3a shows the temperature-dependent transmittance for the star-block copolymer $(DMA_{130}DEGMA_{140})_6$ at different pH values. As a comparison, the linear PDMA homopolymer has an apparent pK_a value of 6.2.[29] At pH 7, when the cloud point of the PDMA block is around 80 °C,[29] both transitions are visible but strongly separated, with the transition of the PDEGMA block at 24 °C, lower than the cloud point of linear PDEGMA homopolymer.[30] The shift of the transition temperature for the PDEGMA star-block copolymer compared to the homopolymer might be due to the fact that the PDMA block is protonated at this pH and hydrogen bonds are formed between the PDMA and PDEGMA blocks, making the stars less soluble.[40,47]

At pH 8, there are also two distinct steps in the transmittance, the first around 28 °C and the second around 50 °C. Both correspond very well to the cloud points of the respective homopolymers of the different blocks, 26 °C for PDEGMA homopolymer[30,31] and around 50 °C for PDMA homopolymer at pH 8.[27,29] All star polymers show this behavior. Fig. 3b compares the transition temperatures of all synthesized star-block copolymers at various pH values. This agrees with the supposed aggregation mechanism (Scheme 1), *i.e.*, a sequential collapse of the blocks takes place upon heating, beginning with the outer PDEGMA block. In dilute solution this leads to the formation of small aggregates. If the temperature is increased further, then, depending on the pH value, the inner PDMA block can collapse, too, leading to precipitation.

However, at pH 9 the cloud point of PDMA is shifted to lower values, around 30 °C,[29] and the block is almost completely deprotonated, making it hydrophobic, which lowers the cloud point of the PDEGMA block.[47] Therefore, the first drop in transmittance observed for $(DMA_{130}DEGMA_{140})_6$ is also attributed to the PDEGMA block (Fig. 3a). This drop continues to almost zero before a small shoulder appears around 27 °C,

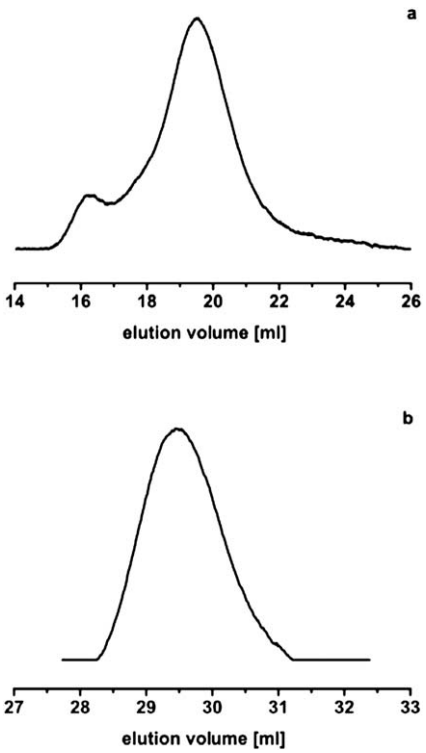

Fig. 2 SEC traces for (a) $(DMA_{150}DEGMA_{100})_4$ in DMAc and (b) the corresponding cleaved off arms, transformed to PMMA and measured in THF.

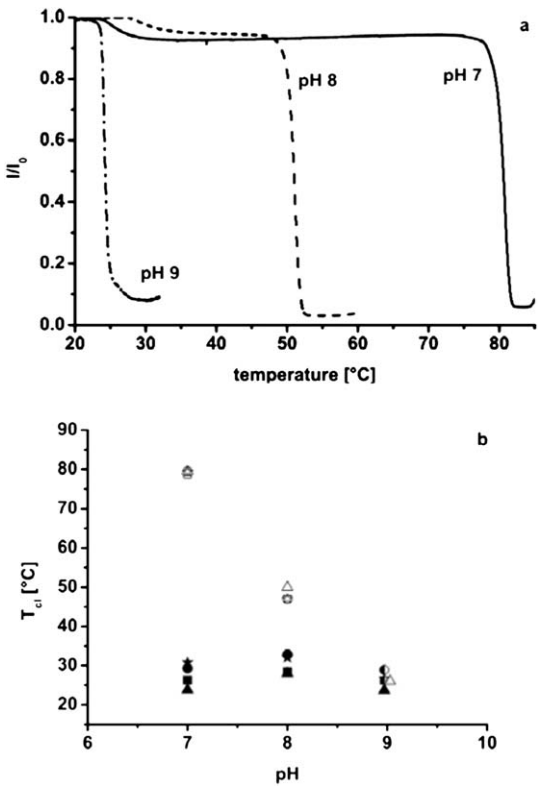

Fig. 3 Turbidity measurements of (a) $(DMA_{130}DEGMA_{140})_6$ and (b) transition temperatures of all stars at different pH values with the open symbols representing the inner PDMA block and the filled symbols the transition temperature of the outer PDEGMA block. (●, ○) $(DMA_{150}DEGMA_{40})_4$; (■, □) $(DMA_{150}DEGMA_{100})_4$; (★, ☆) $(DMA_{130}DEGMA_{60})_6$ and (▲, △) $(DMA_{130}DEGMA_{140})_6$. Half-filled symbols indicate that no distinction between the blocks could be made.

indicating the collapse of the PDMA block and thus complete collapse of the star. This sequence of collapses is confirmed by μDSC measurements (Fig. S2†), showing that the transition of the PDEGMA block occurs before the transition of the PDMA block. This behavior reveals that the blocks can be triggered independently from each other and the diblock copolymer stars can be mono or dual stimuli responsive depending on the pH. However, this is only true for $(DMA_{130}DEGMA_{140})_6$ as the μDSC measurements for the other stars show that the transitions of the two blocks overlap.

To further study the aggregation behavior of the stars, dynamic light scattering experiments (DLS) were carried out. Fig. 4 shows the results for $(DMA_{130}DEGMA_{140})_6$ at pH 7 and 8. In both cases the apparent hydrodynamic radius, $R_{h,app}$, has a value of 19 nm at low temperatures, which is consistent with unimolecularly dissolved stars. Beginning at temperatures above 20 °C, $R_{h,app}$ increases until a maximum is reached at 30 °C. These maxima are 34 and 29 nm for pH 7 and 8, respectively. The increase in size is in line with the collapse of the outer PDEGMA block and the formation of small flower-like aggregates (Scheme 1). At the same time as the size increases the polydispersity index (PDI) of the detected species decreases sharply. This is further evidence for the formation of defined aggregates. The transition temperature is lower than the one determined from turbidity measurements but that is due to the higher sensitivity of the DLS setup, which enables it to detect even small changes in size. At pH 7, $R_{h,app}$ shows a slight decrease from above 30 °C up to 60 °C, but no large aggregates because we cannot reach the transition point of PDMA at ~80 °C (ref. 29) in our experimental setup. The decrease of the radius can be explained by the contraction of the PDMA block due to increased hydrophobicity at elevated temperatures, because the strength of the hydrogen bonds decreases steadily.

At pH 8, $R_{h,app}$ starts to increase at 25 °C, then decreases above 30 °C before rising again above 40 °C and finally reaching values higher than 100 nm for temperatures over 50 °C. The PDI matches this behavior, decreasing between 25 and 30 °C and then increasing again at 50 °C. First, the PDEGMA block starts collapsing above 25 °C and small flower-like aggregates are formed at 30 °C, resulting in the decrease of the PDI. Between 30 and 40 °C, the inner PDMA block contracts because of the decreasing solvent quality close to its cloud point. However, the flower-like aggregates are stable as indicated by the constant low PDI in this region. At 50 °C the PDMA block reaches its aggregation temperature and collapses, causing intermolecular aggregation as seen by the rapid increase of $R_{h,app}$ and PDI over the remaining measurement, *i.e.*, larger and more ill-defined aggregates are formed as the star-block copolymers aggregate into clusters. This behavior agrees with our assumptions for dual temperature and pH responsiveness (Scheme 1). The DLS measurements of the remaining star-block copolymers are shown in Fig. S3†. Their behavior mostly agrees with the one discussed above, except for the star $(DMA_{150}DEGMA_{40})_4$, which has a low arm number and the lowest molar fraction of DEGMA units (21%). The star shows a very broad transition at both pH values, indicating a less defined aggregation. One possible explanation is that due to the small fraction of DEGMA units, stable aggregates are only formed at higher temperatures. This is most pronounced at pH 7, where the PDMA block is hydrophilic and impedes aggregate formation. This would suggest that a minimum fraction of the collapsing outer block is needed to spontaneously form stable aggregates.

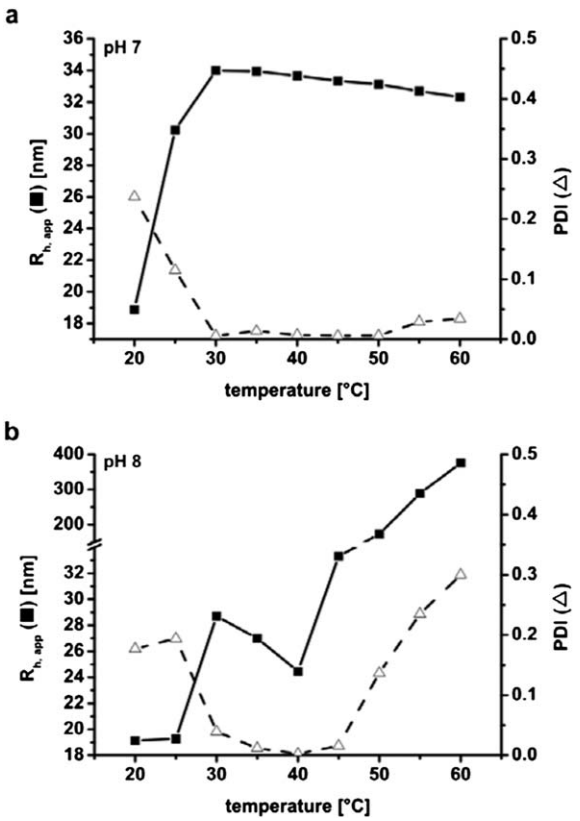

Fig. 4 Temperature-dependent apparent hydrodynamic radii and polydispersity indices derived from cumulant analysis of $(DMA_{130}DEGMA_{140})_6$ at (a) pH 7 and (b) pH 8. Measurements were performed in buffer solutions at 1 g L^{-1} and $\theta = 90°$.

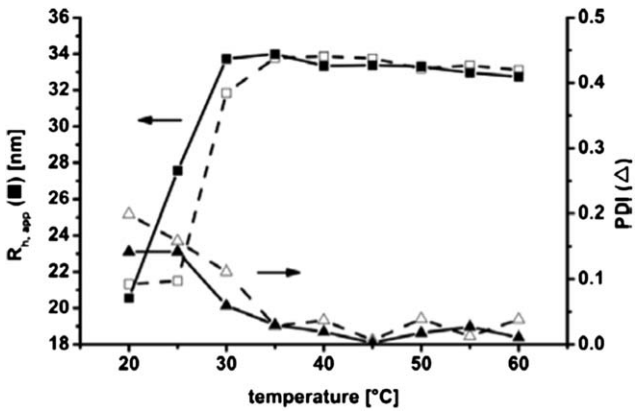

Fig. 5 Temperature-dependent apparent hydrodynamic radii (■, □) and polydispersity indices (▲, △) derived from cumulant analysis of $(qDMA_{130}DEGMA_{140})_6$ at pH 7 (filled symbols) and pH 8 (open symbols). Measurements were performed in buffer solution at 1 g L^{-1} and $\theta = 90°$.

Aggregation of quaternized $(qDMA_nDEGMA_m)_x$ diblock copolymer stars in dilute solution

Through quaternization PDMA becomes a strong polyelectrolyte but loses its sensitivity to temperature and pH. Thus the inner block is no longer stimuli-responsive and the diblock copolymer stars can only undergo one transition independent of the pH value, *i.e.*, the formation of flower-like aggregates upon the collapse of the PDEGMA block. These aggregates should be stable at elevated temperatures due to the polyelectrolyte nature of the inner block. Fig. 5 shows the results for $(qDMA_{130}DEGMA_{140})_6$.

At pH 7, $R_{h,app}$ increases above 20 °C and reaches the same plateau value of 34 nm as the nonquaternized diblock star (Fig. 4 and 5). The value then stays almost constant within the investigated temperature range. Coinciding with this increase in radius is again a decrease of the PDI, supporting the assumption that the PDEGMA block collapses and small flower-like aggregates are formed which are stable even at elevated temperatures. The results for pH 8 are practically equal to those at pH 7, as expected because the inner PqDMA block has no LCST anymore. Hence, the aggregation behavior of the quaternized stars is markedly different to that for the nonquaternized stars as there is only one temperature induced transition visible between 20 and 30 °C.

The results obtained from turbidity measurements and DLS experiments prove the double stimuli responsive nature of the diblock copolymer stars in dilute solutions and that the outer block can be triggered independently of the inner block. This behavior should lead to hydrogel formation in concentrated solutions upon heating, independent of the solution pH as long as the outer block collapses first. To investigate the behavior of the diblock stars in concentrated solutions, tube-inversion experiments and rheology measurements were performed.

Gel formation of $(DMA_nDEGMA_m)_x$ diblock copolymer stars at pH ≈ 8

All samples were prepared by dissolving the polymers in water of appropriately low pH to obtain the desired pH value close to 8, because here the transition temperature of PDMA is in the accessible temperature range (~50 °C).[29] Thus, gel formation is supposed to take place triggered by the collapse of the outer PDEGMA block and upon reaching the transition temperature of the inner PDMA block, the mechanical properties of the gel should change because of the contraction of the PDMA block (Scheme 1). Tube-inversion revealed that at pH values around 8 all the stars, except the one with the lowest PDEGMA fraction, $(DMA_{150}DEGMA_{40})_4$, formed free-standing hydrogels starting from 15 wt%. $(DMA_{150}DEGMA_{40})_4$ does not form gels at any concentration and pH value tested. DLS showed that this star has a very broad transition in dilute solution, making it likely that the physical crosslinks initially formed by this star are not strong enough to enable gelation. On the other hand, the star with the highest DEGMA fraction, $(DMA_{130}DEGMA_{140})_6$, forms free-standing gels even at concentrations as low as 10 wt%.

To obtain a more detailed picture of the gelation behavior of the block copolymer stars selected samples were investigated by rheology. We applied an oscillatory stress to the sample using a cone–and–plate shear cell geometry. Regimes where the storage modulus, G', exceeds the loss modulus, G'', are defined as the gel state according to the common definitions. The sol state is defined

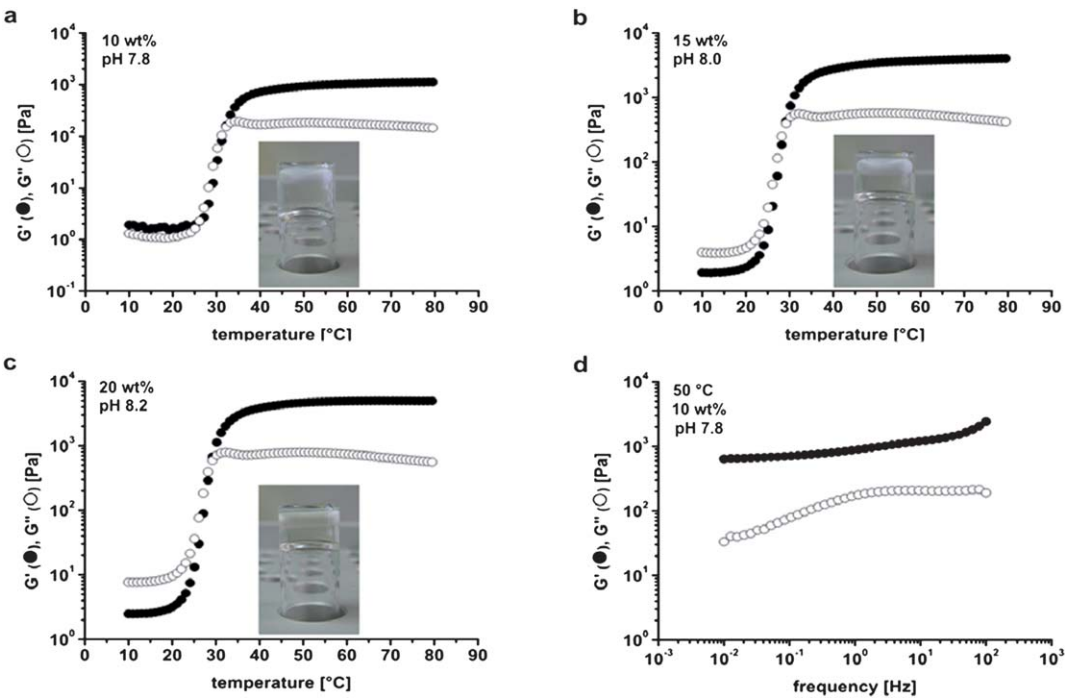

Fig. 6 Temperature-dependent storage and loss moduli for $(DMA_{130}DEGMA_{140})_6$ in (a) a 10 wt% solution at pH 7.8, (b) a 15 wt% solution at pH 8.0, and (c) a 20 wt% solution at pH 8.2 and (d) isothermal frequency sweep at 50 °C for the 10 wt% sample. Insets depict digital photographs of tube-inversion experiments of the respective samples at 50 °C.

by $G' < G''$, and $G' > 1$ kPa is taken as a characteristic value for strong, free-standing gels.[48–50] The point at which G' and G'' intersect is defined as the sol–gel transition temperature, T_{sg}.

Fig. 6 shows typical plots of the temperature-dependent storage and loss moduli for $(DMA_{130}DEGMA_{140})_6$ at different concentrations and one isothermal frequency sweep. At temperatures below 25 °C G'' exceeds G' and the solution is in the sol state, as both blocks are beneath their transition temperature and thus fully soluble in water. With increasing temperature both moduli increase and at 30 °C, the transition temperature of PDEGMA, the solution crosses into the gel state. Eventually G' reaches a plateau with $G' > 1$ kPa, indicating a strong gel (Table 2). This is supported by Fig. 6d, which shows the frequency dependent measurement at 50 °C for the sample depicted in Fig. 6a. G' is higher than G'' over the whole measured frequency range, proving that free-standing gels are formed. Increasing the polymer concentration from 10 wt% to 20 wt% (Fig. 6a–c) leads to a substantial increase in the gel strength because the number of physical crosslinks in the gel increases accordingly. Unexpectedly, the moduli show no change when the temperature is increased above 50 °C, the transition temperature of PDMA, which is attributed to the high gel strength ($G' > 1$ kPa).

Table 2 summarizes the results of the rheology experiments for all measured samples of the star-block copolymers and the corresponding plots of G' and G'' can be found in Fig. 6–8 and S5–S7†. There are some general trends noticeable. The first trend is that an increase in the polymer concentration results in a strengthening of the hydrogels. The second important characteristic is the molar fraction of DEGMA units, f_{DEGMA}, which plays a very important role in the formation of hydrogels for these diblock copolymer stars. As mentioned above, $(DMA_{150}DEGMA_{40})_4$ does not form any hydrogels under the conditions investigated. This leads to the conclusion that a minimum f_{DEGMA} is necessary for hydrogel formation, but most importantly, f_{DEGMA} controls the sol–gel transition temperature (Table 2). Turbidity measurements show that the cloud point decreases with the PDEGMA block length, thus T_{sg} should decrease accordingly. The gel strength on the other hand, is influenced by both f_{DEGMA} and the arm number of the star. This is reasonable, as f_{DEGMA} is proportional to the block length of the PDEGMA block and a longer hydrophobic block leads to stronger gels. The arm number determines the number of possible crosslinking points so that a higher arm number means more crosslinking points and thus a stronger gel. However, the effect of the arm number is more pronounced, as the 6-arm star with the lowest f_{DEGMA} forms stronger gels than the 4-arm star with a higher f_{DEGMA} at all concentrations measured. This suggests that the concentration of crosslinking points is more important than the strength of the hydrophobic interactions. The transition temperature of the inner PDMA block is around 50 °C for pH values around 8, so we expected the dynamic-mechanical behavior of the gels to change upon heating above 50 °C but there is no visible change in G' and G'' for the investigated hydrogels (Fig. 6 and S5†). The high strength of the gels around pH 8 makes them too rigid to respond to the increase in temperature above the transition temperature of PDMA. This is similar to the behavior we observed for gels based on PDMA-*b*-PDEA block copolymer stars.[26] For that reason we decided to investigate gels at higher pH.

Table 2 Gelation behavior of $(DMA_nDEGMA_m)_x$ and $(qDMA_nDEGMA_m)_x$ diblock stars

	f_{DEGMA}[a]	pH[b]	T_{sg}[c] [°C]	G'[d] [kPa]
5 wt%				
$(qDMA_{130}DEGMA_{60})_6$[e]	0.32	Quat.	55	0.73
$(qDMA_{150}DEGMA_{100})_4$[e]	0.40	Quat.	42	0.35
$(qDMA_{130}DEGMA_{140})_6$[e]	0.52	Quat.	36	0.79
10 wt%				
$(qDMA_{130}DEGMA_{60})_6$[e]	0.32	Quat.	53	2.0
$(qDMA_{150}DEGMA_{100})_4$[e]	0.40	Quat.	41	1.0
$(qDMA_{130}DEGMA_{140})_6$[e]	0.52	Quat.	36	1.8
$(DMA_{130}DEGMA_{140})_6$	0.52	7.8	32	1.1
15 wt%				
$(DMA_{130}DEGMA_{60})_6$	0.32	8.2	41	2.8
$(DMA_{150}DEGMA_{100})_4$	0.40	8.2	35	1.7
$(DMA_{130}DEGMA_{140})_6$	0.52	8.0	29	3.9
$(DMA_{130}DEGMA_{140})_6$	0.52	8.8	32	0.07 (0.27[f])
20 wt%				
$(DMA_{130}DEGMA_{60})_6$	0.32	8.3	40	2.8
$(DMA_{150}DEGMA_{100})_4$	0.40	8.4	34	1.9
$(DMA_{130}DEGMA_{140})_6$	0.52	8.2	29	5.0
$(DMA_{130}DEGMA_{140})_6$	0.52	8.7	31	0.13 (0.55[f])

[a] Molar fraction of DEGMA units. [b] Solution pH measured before rheology. [c] Sol–gel transition temperature, defined as the temperature when G' and G'' crossover. [d] Value of G' in the plateau region taken at 70 °C. [e] The degree of quaternization is 85–88%. [f] Value at maximum.

Gel formation of $(DMA_nDEGMA_m)_x$ diblock copolymer stars at pH ≈ 9

Fig. 7 shows the results of the rheology measurements of $(DMA_{130}DEGMA_{140})_6$ at pH values close to 9. The increase of the pH value has two consequences: first, the cloud point of the PDMA block is lowered to around 30 °C and second, the PDMA chains are less stretched because the PDMA blocks are less protonated. The lower degree of protonation together with the contraction of the chains causes a decrease of the effective volume fraction of the stars, making the gels at high pH softer compared to the gels at lower pH values. Again, gelation occurs around 30 °C. Both samples have a lower maximum value of G' compared to their counterparts at pH ≈ 8. The difference in the behavior at pH ≈ 8 becomes visible immediately after the crossover (Fig. 7). G' decreases after reaching a maximum at 35 °C (for 15 wt%) and 40 °C (for 20 wt%) before leveling off again at $T > 60$ °C. This indicates a further contraction of the PDMA block after gelation because the solvent quality of the water decreases steadily with increasing temperature, making this gel dual responsive in its formation process and its mechanical properties in the gel state. The contraction of the chains is in agreement with the behavior of the PDMA blocks at elevated temperatures in DLS. However, since the polymer is already in the gel state the PDMA blocks cannot completely collapse, which leads to the plateau of G' at elevated temperatures.

In contrast, $(DMA_{150}DEGMA_{100})_4$ and $(DMA_{130}DEGMA_{60})_6$ do not form a gel under these conditions ($G'_{max} < 10$ Pa, Fig. S6†). A possible explanation is that $(DMA_{130}DEGMA_{140})_6$ is the only star where the turbidity and μDSC measurements show two distinct transitions even at pH 9 (Fig. 3b and S2a†). The transition temperatures of the PDMA blocks of the other stars coincide with

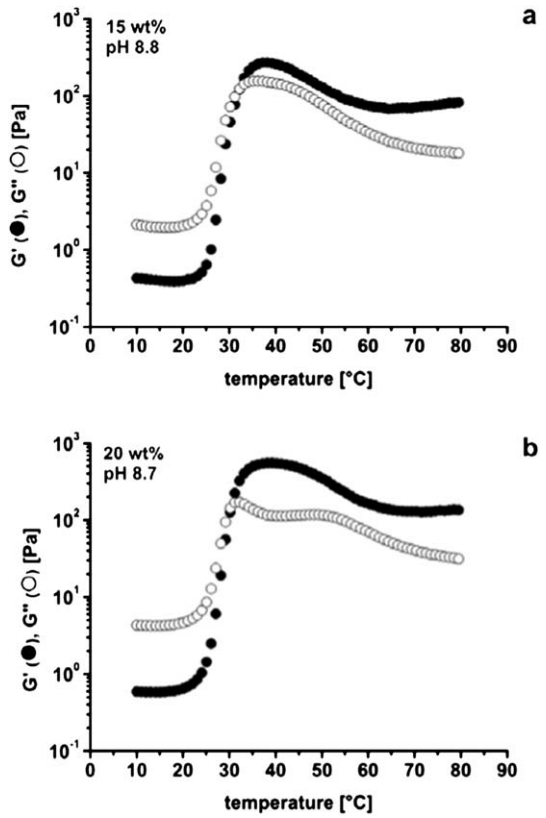

Fig. 7 Temperature-dependent storage and loss moduli for $(DMA_{130}DEGMA_{140})_6$ in (a) a 15 wt% solution at pH 8.8 and (b) a 20 wt% solution at pH 8.7.

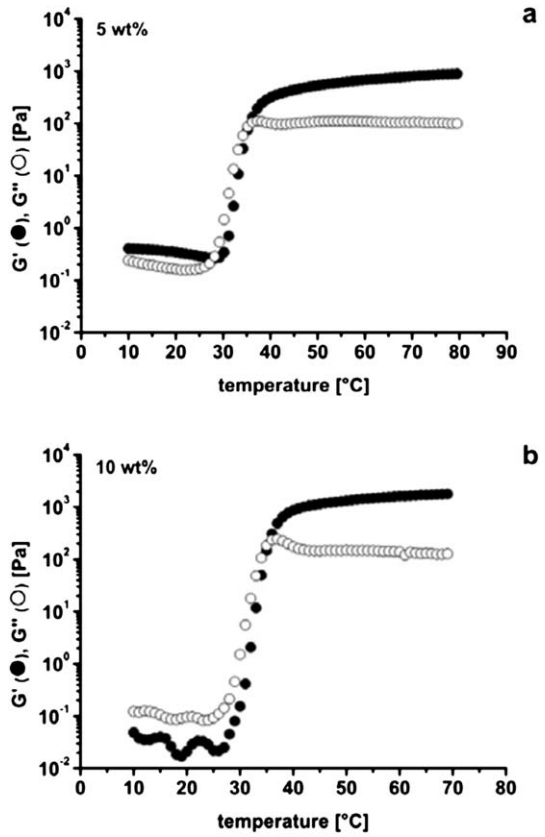

Fig. 8 Temperature-dependent storage and loss moduli for (a) a 5 wt% solution and (b) a 10 wt% solution of $(qDMA_{130}DEGMA_{140})_6$.

those of the PDEGMA blocks, making successful hydrogel formation impossible (Fig. 3b and S2b†). The measurements depicted in Fig. S6† all show an increase in G' around 30 °C, the transition temperature of PDEGMA, but before a gel can be formed the moduli drop sharply. This is attributed to the collapse of the PDMA block shortly after the PDEGMA block has collapsed. In these cases stable crosslinking points cannot be formed, making network formation impossible.

Gel formation of quaternized $(qDMA_nDEGMA_m)_x$ diblock copolymer stars

In this system hydrogel formation takes place upon the collapse of the outer PDEGMA block, the same as for the non-quaternized diblock copolymer stars. The resulting gels will not be dual stimuli responsive as the thermo- and pH-responsiveness of the inner PDMA block is lost upon quaternization. This prediction is confirmed by both tube inversion and rheology measurements. Tube-inversion experiments show a significant decrease of the critical gelation concentration as compared to the nonquaternized stars. As an example, gel formation for $(qDMA_{130}DEGMA_{140})_6$ takes place at concentrations as low as 2 wt%. This is due to the increased stretching of the PqDMA block because of the much higher charge density and the increased osmotic pressure of the counterions. However, the rheology measurements of $(qDMA_{130}DEGMA_{140})_6$ show that the gels formed at 5 wt% and lower cannot be categorized as strong free-standing gels but rather are considered to be soft gels ($G' < 1$ kPa).

Fig. 8 shows the rheology measurements of $(qDMA_{130}DEGMA_{140})_6$ at concentrations of 5 wt% and 10 wt% and the other quaternized stars are shown in Fig. S7†. In Fig. 8 a sol–gel transition is observed upon heating the samples and the storage modulus does not decrease again after reaching the gel state.

An increase in the polymer concentration also leads to a strengthening of the gel analogous to the behavior of the nonquaternized stars. Here, we can directly compare 10 wt% samples of $(DMA_{130}DEGMA_{140})_6$ and $(qDMA_{130}DEGMA_{140})_6$ in terms of sol–gel transition temperature and gel strength (Table 2). Through quaternization, T_{sg} shifts to slightly higher temperatures because of the hydrophilic PqDMA block, *i.e.*, the transition temperature of the PDEGMA block is increased, and the gel strength increases due to the higher effective volume fraction of the quaternized stars. The behavior of the quaternized stars is similar to that of the nonquaternized stars, insofar as T_{sg} is solely controlled by f_{DEGMA} and the gel strength is mainly controlled by the arm number of the stars and to a lesser extent by f_{DEGMA}.

Conclusions

Turbidimetry and dynamic light scattering have confirmed that $(DMA_nDEGMA_m)_x$ diblock copolymer stars are double-responsive to pH and temperature in dilute aqueous solution. Upon heating the outer PDEGMA block collapses first and

flower-like aggregates are formed. When the temperature is increased further, the inner PDMA block responds depending on the pH value. If the pH is chosen correctly, a sequential collapse starting with the outer block can be triggered. Therefore, in concentrated aqueous solutions, hydrogel formation takes place upon the collapse of the outer PDEGMA block and the mechanical properties of the gel can be manipulated further by temperature. Unexpectedly, the gels formed at pH $\approx$ 8 do not show a change in their moduli when the temperature is increased above the transition temperature of PDMA. This is attributed to the fact that in these cases strong gels are formed ($G'_{max} \geq 1$ kPa), which are too rigid to be affected. However, when the gels are prepared at pH $\approx$ 9 they exhibit significantly reduced gel strength and thus a drop of the moduli upon heating over the transition temperature of PDMA can be observed.

To further prove the versatility of our system, the inner PDMA blocks were quaternized to form PqDMA, a strong polycation. Further advantages of a quaternized block are the possibilities to incorporate nanoparticles or to introduce a light sensitivity through multivalent counterions.[28,51] During the quaternization the temperature and pH responsiveness of the inner block is lost but so are the restrictions on the solution pH value. The increased effective volume fraction of the quaternized diblock stars leads to a significant decrease in the critical gelation concentration.

Acknowledgements

The German Science Foundation is acknowledged for financial support within the priority program SPP 1259. We thank Florian Stegmann for his help in the synthesis, Ingo Rehberg and Reinhard Richter (Experimental Physics V, University of Bayreuth) for providing us with access to their rheometer and Marietta Böhm (Macromolecular Chemistry II, University of Bayreuth) for performing the SEC measurements.

References

1 C. He, S. W. Kim and D. S. Lee, *J. Controlled Release*, 2008, **127**, 189–207.
2 A. S. Hoffman, *Adv. Drug Delivery Rev.*, 2002, **54**, 3–12.
3 C. Alarcon, H. de Las, S. Pennadam and C. Alexander, *Chem. Soc. Rev.*, 2005, **34**, 276–285.
4 E. Ruel-Gariepy and J.-C. Leroux, *Eur. J. Pharm. Biopharm.*, 2004, **58**, 409–426.
5 N. A. Peppas, J. Hilt, A. Khademhosseini and R. Langer, *Adv. Mater.*, 2006, **18**, 1345–1360.
6 T. Okano, N. Yamada, M. Okuhara, H. Sakai and Y. Sakurei, *Biomaterials*, 1995, **16**, 297–303.
7 P. S. Stayton, T. Shimoboji, C. Long, A. Chilkoti, G. Ghen, J. M. Harris and A. S. Hoffman, *Nature*, 1995, **378**, 472–474.
8 J. Zhang and N. A. Peppas, *Macromolecules*, 2000, **33**, 102–107.
9 B. Jeong, S. W. Kim and Y. H. Bae, *Adv. Drug Delivery Rev.*, 2002, **54**, 37–51.
10 A. Kikuchi and T. Okano, *Prog. Polym. Sci.*, 2002, **27**, 1165–1193.
11 C. Tsitsilianis, *Soft Matter*, 2010, **6**, 2372–2388.
12 S.-K. Ahn, R. M. Kasi, S.-C. Kim, N. Sharma and Y. Zhou, *Soft Matter*, 2008, **4**, 1151–1157.
13 L. Yu and J. Ding, *Chem. Soc. Rev.*, 2008, **37**, 1473–1481.
14 C. Li, Y. Tang, S. P. Armes, C. J. Morris, S. F. Rose, A. W. Lloyd and A. L. Lewis, *Biomacromolecules*, 2005, **6**, 994–999.
15 L. Yu, G. Chang, H. Zhang and J. Ding, *J. Polym. Sci., Part A: Polym. Chem.*, 2007, **45**, 1122–1133.
16 M. S. Jones, *Eur. Polym. J.*, 1999, **35**, 795–801.
17 T. G. O'Lenick, N. Jin, J. W. Woodcock and B. Zhao, *J. Phys. Chem. B*, 2011, **115**, 2870–2881.
18 C. Li, N. J. Buurma, I. Haq, C. Turner, S. P. Armes, V. Castelletto, I. W. Hamley and A. L. Lewis, *Langmuir*, 2005, **21**, 11026–11033.
19 S. Sugihara, S. Kanaoka and S. Aoshima, *J. Polym. Sci., Part A: Polym. Chem.*, 2004, **42**, 2601–2611.
20 M. K. Nguyen, D. K. Park and D. S. Lee, *Biomacromolecules*, 2009, **10**, 728–731.
21 S. A. Angelopoulos and C. Tsitsilianis, *Macromol. Chem. Phys.*, 2006, **207**, 2188–2194.
22 F. Bossard, C. Tsitsilianis, S. N. Yannopoulos, G. Petekidis and V. Sfika, *Macromolecules*, 2005, **38**, 2883–2888.
23 S. Reinicke, J. Schmelz, A. Lapp, M. Karg, T. Hellweg and H. Schmalz, *Soft Matter*, 2009, **5**, 2648–2657.
24 N. Fechler, N. Badi, K. Schade, S. Pfeifer and J.-F. Lutz, *Macromolecules*, 2009, **42**, 33–36.
25 H.-H. Lin and Y.-L. Cheng, *Macromolecules*, 2001, **34**, 3710–3715.
26 A. Schmalz, H. Schmalz and A. H. E. Müller, *Z. Phys. Chem.*, 2012, DOI: 10.1524/zpch.2012.0240.
27 F. A. Plamper, A. Schmalz, E. Penott-Chang, M. Drechsler, A. Jusufi, M. Ballauff and A. H. E. Müller, *Macromolecules*, 2007, **40**, 5689–5697.
28 F. A. Plamper, A. Schmalz, M. Ballauff and A. H. E. Müller, *J. Am. Chem. Soc.*, 2007, **129**, 14538–14539.
29 F. A. Plamper, M. Ruppel, A. Schmalz, O. Borisov, M. Ballauff and A. H. E. Müller, *Macromolecules*, 2007, **40**, 8361–8366.
30 A. Hoth and J.-F. Lutz, *Macromolecules*, 2006, **39**, 893–896.
31 Ö. Akdemir, A. Hoth and J.-F. Lutz, *J. Am. Chem. Soc.*, 2006, **128**, 13046–13047.
32 S. Han, M. Hagiwara and T. Ishizone, *Macromolecules*, 2003, **36**, 8312–8319.
33 C. Pietsch, R. Hoogenboom and U. S. Schubert, *Angew. Chem., Int. Ed.*, 2009, **48**, 5653–5656.
34 M. W. Jones, M. I. Gibson, G. Mantovani and D. M. Haddleton, *Polym. Chem.*, 2011, **2**, 572–574.
35 S. Park, H. Y. Cho, J. A. Yoon, Y. Kwak, A. Srinivasan, J. O. Hollinger, H.-j. Paik and K. Matyjaszewski, *Biomacromolecules*, 2010, **11**, 2647–2652.
36 C. Porsch, S. Hansson, N. Nordgren and E. Malmstrom, *Polym. Chem.*, 2011, **2**, 1114–1123.
37 N. Kumano, T. Seki, M. Ishii, H. Nakamura and Y. Takeoka, *Angew. Chem., Int. Ed.*, 2011, **50**, 4012–4015.
38 J. A. Yoon, C. Gayathri, R. R. Gil, T. Kowalewski and K. Matyjaszewski, *Macromolecules*, 2010, **43**, 4791–4797.
39 A. Munoz-Bonilla, M. Fernandez-Garcia and D. M. Haddleton, *Soft Matter*, 2007, **3**, 725–731.
40 S. Reinicke and H. Schmalz, *Colloid Polym. Sci.*, 2011, **289**, 497–512.
41 Y. Li, Y. Tang, R. Narain, A. L. Lewis and S. P. Armes, *Langmuir*, 2005, **21**, 9946–9954.
42 F. A. Plamper, H. Becker, M. Lanzendörfer, M. Patel, A. Wittemann, M. Ballauff and A. H. E. Müller, *Macromol. Chem. Phys.*, 2005, **206**, 1813–1825.
43 A. Schmalz, M. Hanisch, H. Schmalz and A. H. E. Müller, *Polymer*, 2010, **51**, 1213–1217.
44 F. Zeng, Y. Shen and S. Zhu, *Macromol. Rapid Commun.*, 2002, **23**, 1113–1117.
45 A. Jusufi, C. Likos and M. Ballauff, *Colloid Polym. Sci.*, 2004, **282**, 910–917.
46 B. Das, X. Guo and M. Ballauff, *Prog. Colloid Polym. Sci.*, 2002, **121**, 34–38.
47 P. J. Roth, F. D. Jochum, F. R. Forst, R. Zentel and P. Theato, *Macromolecules*, 2010, **43**, 4638–4645.
48 F. Chambon and H. H. Winter, *Polym. Bull.*, 1985, **13**, 499–503.
49 M. Mours and H. H. Winter, *Adv. Polym. Sci.*, 1997, **134**, 165–234.
50 K. Nishinari, *Prog. Colloid Polym. Sci.*, 2009, **136**, 87–94.
51 F. A. Plamper, A. Walther, A. H. E. Müller and M. Ballauff, *Nano Lett.*, 2007, **7**, 167–171.